

Preliminary Design of a Crewed Mission to Asteroid Apophis in 2029-2036

Sam Wagner,^{*} Dan Zimmerman,[†] and Bong Wie[‡]
Asteroid Deflection Research Center-Iowa State University, Ames, IA, USA

A crewed mission to a near-Earth object (NEO) as early as 2025 was announced by President Obama on April 15th, 2010 at the Kennedy Space Center in Florida. This was announced as part of NASA's new space exploration plan after announcing plans to cancel the Constellation program. The extensive requirements of such a mission would help NASA to evaluate the performance of future space systems prior to sending a crewed mission to Mars. Apophis, an asteroid of particular interest due to its once high impact probability, would be a logical choice for a manned mission in the near future. This mission could provide a valuable NEO research opportunity to determine the composition of Apophis. This data that would be extremely useful if Apophis were to pass through the gravitational keyhole in 2029, which would then require a deflection mission. This paper focuses on mission design as well as the system architecture that would be required for this mission to Apophis. The primary mission will be a 180 day mission in the 2028-2029 range during the Earth-Apophis close encounter on April 13th, 2029. In an effort to reduce mission requirements mission analysis for missions up to 1 year will be performed as well. In this paper a crewed mission will be designed for a fictional scenario where Apophis has gone through the 2029 keyhole, which puts it on a resonant orbit that will collide with the earth on April 13th, 2036. This work provides baseline mission requirements and optimum launch windows and trajectories for the crewed mission to Apophis, as well as possible mission architecture that allow such missions.

Nomenclature

a	Semi-major Axis (AU or km)
AU	Astronomical Unit
C_3	Earth Escape Energy (km^2/s^2)
CEV	Crew Exploration Vehicle
e	Eccentricity
EDS	Earth Departure Stage
GTO	Geostationary Transfer Orbit
H	Absolute Magnitude
i	Inclination (deg)
I_{sp}	Specific Impulse (s)
ISV	Integrated Space Vehicle
kT	Kiloton
LV	Launch Vehicle
LEO	Low Earth Orbit
m	Mass (kg)
M	Mean Anomaly Angle (deg)
MJD	Mean Julian Date
mT	Metric Ton
NASA	National Aeronautics and Space Administration
NED	Nuclear Explosive Device
NEO	Near-Earth Object
PHO	Potentially Hazardous Object

^{*}Graduate Research Assistant, Dept. of Aerospace Engineering, 2271 Howe Hall, AIAA Student Member.

[†]Graduate Research Assistant, Dept. of Aerospace Engineering, 2271 Howe Hall, AIAA Student Member.

[‡]Vance Coffman Endowed Chair Professor, Dept. of Aerospace Engineering, 2271 Howe Hall, AIAA Associate Fellow.

OTV	Orbital Transfer Vehicle
RSRM	Reusable Solid Rocket Motor
TCM	Trajectory Correction Maneuver
TLI	Trans-Lunar Injection
ΔV	Change in Velocity (km/s)
θ	True Anomaly (deg)
Ω	Right Ascension of Ascending Node (deg)
ω	Argument of Periapsis (deg)

I. Introduction

The Asteroid Deflection Research Center (ADRC) has been conducting a study to design a crewed mission to an asteroid, for the purpose of asteroid deflection or human exploration of asteroids. This could be done using technologies and launch vehicles currently in development for NASA's current Constellation program or its future replacement program. For this study, the mission analysis will be performed to determine the requirements for up to a 1 year mission in the 2028-2029 range as well as prior to a hypothetical 2036 Apophis impact. Possible configurations using architectures similar to Constellation as well as other possible launch vehicle will be considered for this study.

NASA's Constellation Program, originally developed through the Vision for Space Exploration, lays out a plan to fulfill the goals of the Vision for Space Exploration as well as the 2005 NASA Authorization Act. Through the Constellation Program NASA planned to develop a replacement for the shuttle, as well as the capability to deliver 4-6 crew members to the International Space Station (ISS) or the lunar surface for an extended stay. For the Constellation program, two separate launch vehicles, the Ares I and V, as well as the the Orion CEV and the Altair lunar lander are under development. Using these new launch vehicles NASA planned to complete a manned lunar mission through a dual Ares I and Ares V launch. President Obama in his speech at Kennedy Space Center on April 15th, 2010 has proposed by-passing the lunar mission for a crewed NEO mission by 2025 and a Mars mission approximately 10 years afterwards. This coincides well with the idea of a crewed Apophis mission. Apophis is not a suitable candidate for the first human NEO mission, but could be used as a stepping stone to test equipment and procedures for a future crewed Mars mission.

The idea of a crewed mission to an NEO has been proposed in several studies as far back as the Apollo era in the 1960's.¹⁻¹⁰ In 1966, a study performed at NASA proposed using the Apollo and Saturn V hardware to send a crewed mission to asteroid 433 Eros.⁶ The proposed mission would have taken place in 1975 when 433 Eros passed within 0.15 AU of the Earth. This study also detailed the hardware changes necessary for a 500+ day mission. A later crewed NEO study performed by O'Leary outlined the necessary mission requirements to mine several near-Earth and main-belt asteroids.⁴ The proposed missions required 1-3 years total mission times, well beyond the mission length of any recent crewed NEO studies. Several other studies were performed in the late 1980's as part of the Space Exploration Initiative, however interest in crewed NEO missions declined drastically until recent years.

Interest in crewed NEO missions has again increased as NASA's Constellation Program matures and with President Obama's current plan to bypass the proposed lunar missions for a crewed NEO mission by 2025. Over the past few years, several studies have been conducted to determine the feasibility of using Constellation hardware for a crewed NEO mission for a 45-180 day mission with a 7-14 day asteroid stay time.¹⁻³ The current studies have limited target asteroids to those that have low eccentricities (<0.5) and inclinations (<3.0 deg), have an Earth close approach, slow rotation (rotational periods of 10 hours or longer), and are single solitary objects. These strict limitations result in a mission requiring minimal ΔV and short mission times, generally less than 120 days.

An asteroid on a collision course with the Earth may not fit into these very narrow restrictions that recent crewed NEO studies have imposed. This is the reason why the ADRC has been developing the software necessary to help determine the feasibility of such a mission, from a mission analysis perspective, as well as possible mission architectures. The asteroid 99942 Apophis is one such asteroid and will be used as the reference asteroid for this study. A crewed mission to Apophis, which has a relatively low eccentricity of 0.1912 and an inclination of 3.3314 deg, requires a total ΔV 12 km/s for a 180 day mission (the longest allowed under the current NASA crewed NEO studies). Decreasing the mission length increases the required ΔV , the opposite is also true. This is well beyond the reach of the most proposed crewed NEO studies, which require a total ΔV of less than 7 km/s. It is because of the strict limitations of recent crewed NEO studies that the ADRC has decided to examine the feasibility of a crewed Apophis mission as well as to determine possible mission architectures. Such a mission may also be an appropriate step between the first crewed NEO and Mars missions.

Table 1. Characteristics of Apophis

Characteristic	Value	Unit
Epoch	6/18/2009	
a	0.9224	AU
e	0.1912	
i	3.3314	deg
Ω	204.4425	deg
ω	126.4042	deg
θ_0	134.7126	deg
Orbit Period	323.5969	d
Rotational Period	30.5	h
Diameter	270	m
Mass	2.70e10	kg
Escape Velocity	0.1389	m/s
Albedo	0.33	
Absolute Magnitude H	19.7	

According to NASA/JPL's estimates Apophis has a 270 meter diameter and could generate over 500 mega-tons of energy if an impact with the Earth were to occur. This impact would be over 100 times larger than the Tunguska impact in 1908. A list of all the known orbital elements and physical properties of Apophis are given in Table 1.^{11,12}

On April 13th, 2029 Apophis will pass between 5.62 and 6.2 Earth radii (35845-40182 km), well within geostationary orbit. If Apophis were to pass through a 600 meter keyhole, within the orbital uncertainty, it will enter a resonant orbit and impact the Earth on April 13th, 2036. NASA has predicted approximately a 4-in-a million chance that Apophis will pass through the keyhole in 2029. A list of orbital elements that result in 2036 impact are shown in Table 2. Mission analysis for a crewed mission will be performed for both the 2029¹⁰ and hypothetical 2036 close Earth-Apophis encounters. Details on the methods and algorithms used to design the mission analysis search program can be found in Appendices A and B.

Table 2. Orbital and physical data used for a fictive post-2029 asteroid Apophis mission.¹³

Elements	Value
epoch MJD	64699
a, AU	1.108243
e	0.190763
i, deg	2.166
Ω , deg	70.23
ω , deg	203.523
M_0 , deg	227.857

“The problem is acute enough for Apophis that, if impact hasn't been previously excluded, AND there hasn't been a thorough physical characterization, it can't be known for certain it will impact until during or after the 2029 encounter, even if a spacecraft is accompanying Apophis and providing position measurements good to 2 meters. That is, the keyhole could be determined only retrospectively, after passage through it.”¹¹

II. Mission Analysis

To determine the feasibility of a manned mission to Apophis, the mission requirements must be determined. In particular the minimum ΔV necessary to complete the mission and the accompanying launch windows must be found. A computer program has been developed at the ADRC, which combines Lambert solvers with ephemeris data and various other functions to search for launch opportunities, find the required ΔV for each separate maneuver, and plot

interplanetary trajectories. The program performs a search to find the minimum ΔV for each launch date by checking, in 1 day time-steps all the possible Apophis arrival, and departure date combinations. Only the desired mission length and a range of launch dates to search needs to be specified by the user. For the following analysis a 185 km circular parking orbit is assumed to be the departure point. To help minimize the total required ΔV the atmospheric entry speed is limited to a maximum of 12 km/s. Throughout this entire study an Apophis stay time of 10 days is assumed. The total mission ΔV can be lowered slightly by decreasing the total stay time. Depending on the final CEV re-entry velocity a skip re-entry may be necessary. The results obtained using this program for both the 180 and 365 day missions to Apophis near the 2029 encounter as well as a crewed mission prior to the 2036 impact will be analyzed.

A. 2028-2029 Launch Opportunities

For an NEO return mission, two possible launch dates near the Earth-asteroid close encounter always exist. One launch always returns to the Earth near the Earth-Apophis encounter date, while the other launch date occurs on the date of the close encounter. Throughout the rest of the analysis the launch prior to the Earth-Apophis close encounter will be referred to as the early launch date/window, while the launch occurring near the close encounter will be referred to as the late launch date/window.

A plot of the total ΔV required for both the early and late launch dates versus mission length (ranging from 20 to 365 days) is shown in Figure 1.⁹ As shown in Figure 1, the total ΔV is, in general, reduced as the length of the mission increases. Figure 1 shows that a local minimum for the required total ΔV occurs near the 180 day mission length. Current crewed NEO studies have limited the maximum mission length to 180 days for supply and maximum radiation dose limitations. Therefore a complete mission analysis and launch window search for a 180 day mission length, results in a required ΔV in the 10-11 km/s range. Lowering the total mission length may be possible depending on the possible mission architecture and ΔV capabilities.

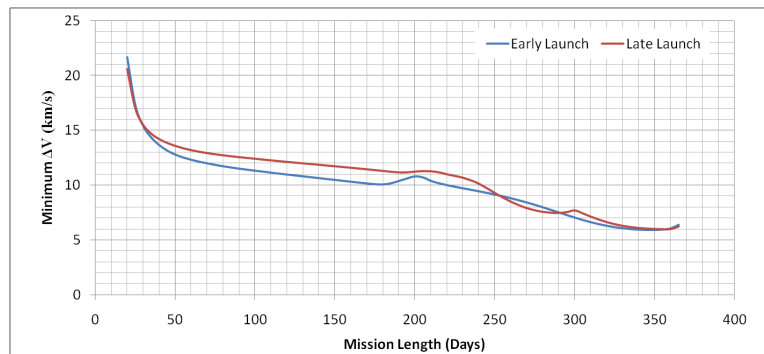


Figure 1. Plot of mission length versus minimum ΔV required to the early and late launch.

1. 180-Day Mission Analysis

With a total mission length selected further analysis can be performed to find the dates and length of each launch window. This can be obtained by calculating the minimum launch ΔV for launch dates near the Earth-Apophis encounter. This information is shown in Figure 2, which is a plot of launch dates versus the total required ΔV for the selected 180 day mission. As previously mentioned the first launch date occurs approximately 180 days prior to the April 13th, 2029 Apophis encounter, while the late launch date occurs on April 13th.

Further examination of Figure 2 reveals that the launch window may be the last opportunities to launch a quick return mission to Apophis. Any manned missions to Apophis after the April 13th, 2029 launch date would likely require significantly increased mission times, possibly even multiple revolutions around the sun before rendezvous, to reduce the required ΔV to an obtainable amount. A mission of this length would likely require significant modifications to the Orion spacecraft to allow for greater radiation shielding and amount of supplies carried. For a short quick return mission to Apophis the April 13th, 2029 launch is the last easily obtainable launch date.

Limiting the maximum allowable launch ΔV to 11.5 km/s allows for sufficiently large launch windows. The minimum ΔV capability requirements for the mission are determined by allowing for a 0.5-1 km/s error margin. Adding this error margin to the maximum allowable launch ΔV results in a required ΔV capability of 12-12.5 km/s.

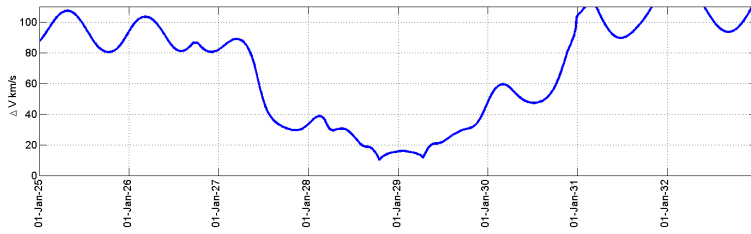


Figure 2. Launch date(2028-2038) versus minimum ΔV required for 180 day return mission.

Using this 11.5 km/s limit the launch windows can be found for both launch dates. The launch windows are then found by limiting the plot in Figure 2 to the 2028-2029 time frame. The resulting graph is shown in Figure 3, which has the total ΔV plot as well as the required ΔV for the Earth departure, Apophis arrival, Apophis departure, and Earth arrival burns. As Figure 3 shows, the early launch window is approximately 12 days starting on Oct. 12, 2028 and ending on Oct. 24, 2028. The late launch window is significantly shorter at just over 2 days in length, ranging from Apr. 12-14, 2029.

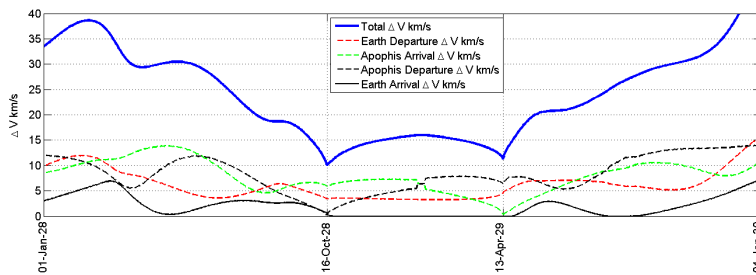


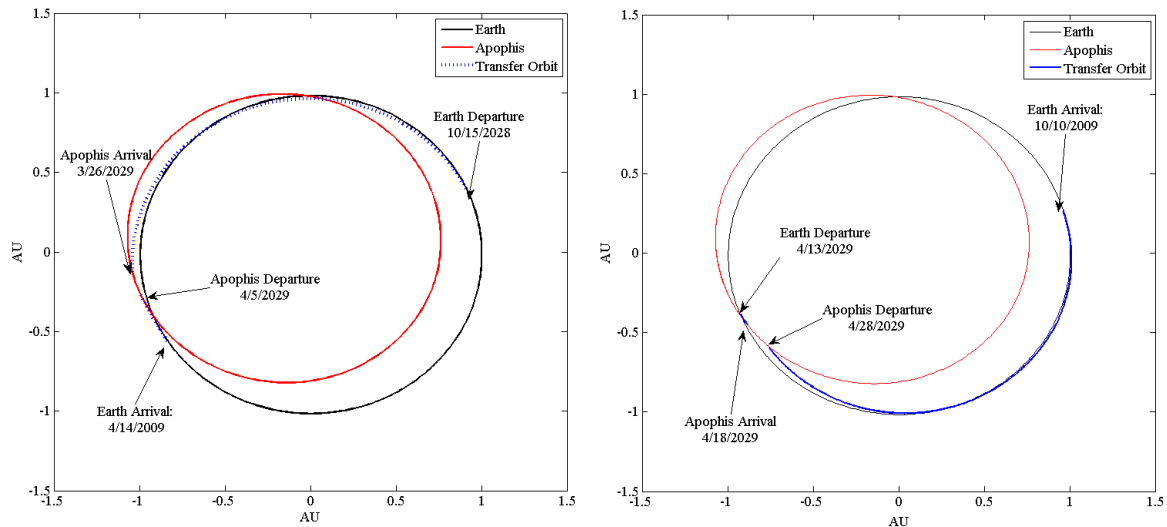
Figure 3. Launch windows found in the 2028-2029 time frame. Plot of launch date versus minimum total ΔV required.

A summary of nominal launch dates for both launch opportunities is shown in Table 3. The dates for each maneuver as well as the ΔV magnitude and C_3 values are given for each maneuver. For the early launch date all of the maneuvers, with the exception of the Earth departure burn, are carried out in the last 3 weeks of the mission. The return date for the early launch date is just after the Apr. 13th, 2029 Earth-Apophis encounter, which allows for a small return ΔV because the Orion spacecraft departs Apophis a few days prior the the Earth-Apophis encounter. The opposite is true for the late launch date. Earth departure occurs during the Earth-Apophis close approach, with the Apophis rendezvous occurring a few days after Earth departure. Within the first 2-3 weeks the mission is completed, with the remaining time spent on the return cruise. No burn is necessary when the Orion spacecraft returns to the Earth because the atmospheric reentry speed is less than 12 km/s.

2. 365 Day Mission Analysis

From Figure 1 it is clear that longer missions result in significantly lower ΔV requirements. It can be seen that extending the mission to 1 year in length results in a mission requiring a total ΔV of 6-7 km/s, significantly lower than the 10-12 km/s require for a 180-day mission. Such a mission could likely be executed using the standard Constellation or similar mission architecture. This mission would likely be used as a stepping stone between the first asteroid mission, in the 2025 time frame, and the first Mars flyby mission, to occur in the 2035 time frame. This mission could serve as a test bed for systems needed for a Mars flyby or landing mission, with a reduced mission time when compared to a Mars mission.

A plot of the total ΔV needed for 2028-2029 time frame missions can be seen in Figure 5. Figure 5 shows the total ΔV needed for both the early and late launch date is just under 6.5 km/s, which may allow for a single launch of Ares V class of launch vehicle carrying a CEV such as the Orion crewed capsule. Both launch windows can be determined by limiting the total ΔV to 7 km/s. The early launch window has a length of 27 days lasting from from April 12th,



(a) Early launch mission trajectory. Sun centered J2000 coordinate system. (b) Late launch mission trajectory. Sun centered J2000 coordinate system.

Figure 4. Early and late mission trajectories.

2028 to May 9th, 2028. The second launch window is slightly longer at 35 days, ranging from March 11th, 2036 to April 15th, 2036.

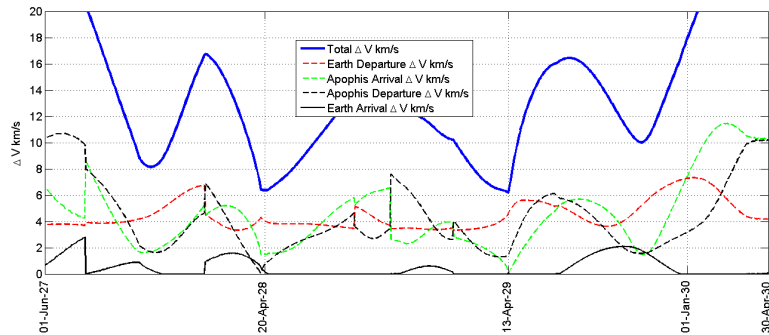


Figure 5. Launch windows found in the 2028-2029 time frame. Plot of launch date versus minimum total ΔV required.

A summary of the two nominal launch dates is shown in Table 4. The dates for each maneuver as well as the ΔV magnitude and C_3 values are given for each maneuver as well. For the early launch date all of the maneuvers, with the exception of the Earth departure burn, are carried out in the last 2 months of the mission. The return date for the early launch date is just after the Apr. 13th, 2029 Earth-Apophis close encounter, which allows for a small return ΔV because the CEV departs Apophis a few days prior to the Earth-Apophis encounter. The opposite is true for the late launch date. Earth departure occurs during the Earth-Apophis close approach, with the Apophis rendezvous occurring a few days after Earth departure. Within the first 4-5 weeks the mission is completed, with the remaining time spent on the return cruise. In each case a burn is necessary when the CEV returns to the Earth because of the required atmospheric reentry speed of 12 km/s or less.

B. Launch Opportunities Prior to 2036 Impact

This section provides an outline of the mission requirements necessary for an asteroid deflection mission prior to impact on April 13th, 2036. This was done by ensuring that the Apophis departure date occurs on or before the impact

Table 3. Mission information for each launch opportunity for the 180 day missions.

Mission Information	Early Launch	Late Launch
Earth Departure		
Date	16-Oct-2028	13-Apr-2029
C_3	4.887	30.355
ΔV (km/s)	3.448	4.528
Apophis Arrival		
Date	26-Mar-2029	19-Apr-2029
V_∞^2	34.504	0.136
ΔV (km/s)	5.874	0.369
Apophis Departure		
Date	5-Apr-2029	29-Apr-2029
C_3	0.113	40.686
ΔV (km/s)	0.336	6.379
Earth Arrival		
Date	14-Apr-2029	10-Oct-2029
V_∞^2	30.474	1.896
ΔV (km/s)	0.391	0.000
Re-Entry V (180 km alt)	12.000	11.111
Total ΔV (km/s)	10.049	11.276

date. All figures and tables in this section represent this requirement. For this mission there is no equivalent launch date for what was referred to as the late launch.

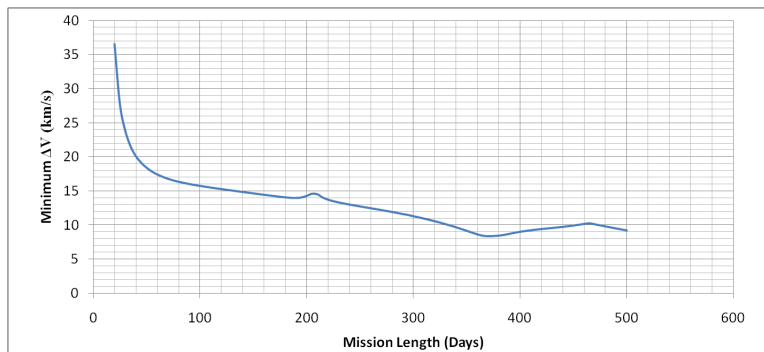


Figure 6. Plot of mission length versus minimum ΔV required to the 2036 crewed deflection mission.

A plot of minimum ΔV for mission lengths from 20 to 500 days is shown in Figure 6. Examination of Figure 6 reveals that there is a minimum required ΔV of just under 8.5 km/s. A 180 day mission requires a ΔV of over 14 km/s, which is not feasible given current space propulsion technology. The 12 km/s ΔV required for a 180 day mission in 2029 is very difficult to achieve and would likely involve the use of orbital transfer vehicles that currently don't exist. This would be inappropriate for an Apophis deflection mission, where the livelihood of so many people is at stake. For this reason, the only mission analysis performed in this section will be a 365 day mission, which is near the minimum total ΔV shown in Figure 6.

From Figure 7 it can be seen that there is only one minimum, which occurs approximately one year prior to impact of the fictional Apophis. This same plot is shown in more detail closer to the launch date in Figure 8. This plot shows the ΔV values for each maneuver as well. Limiting the total ΔV to 9 km/s allows for a 2 week launch window starting on April 11th, 2035 and ending on April 25th, 2036. Depending on the specific architecture chosen this windows may be adjusted.

A complete summary of the nominal launch date shown in Figure 8 is provided in Table 5. The dates and ΔV

Table 4. Mission information for each launch opportunity for the 365 day missions.

Mission Information	Launch 1	Launch 2
Earth Departure		
Date	20-Apr-2028	13-Apr-2029
C3	18.025	30.762
ΔV (km/s)	4.017	4.545
Apophis Arrival		
Date	21-Feb-2029	11-May-2029
V_{∞}^2	2.211	0.065
ΔV (km/s)	1.487	0.255
Apophis Departure		
Date	3-Mar-2029	21-May-2029
V_{∞}^2	0.546	1.946
ΔV (km/s)	0.739	1.395
Earth Arrival		
Date	20-Apr-2029	13-Apr-2030
V_{∞}^2	24.053	21.269
ΔV (km/s)	0.129	0.014
Re-Entry V (180 km alt)	12.000	12.000
Totals		
ΔV (km/s)	6.373	6.208

magnitudes for each maneuver, as well as C_3 and other information needed. For this mission the majority of the maneuvers, with the exception of the Earth departure burn, occur within that last 43 days of the mission. The Earth arrival date occurs just after the April 13th, 2036 impact, assuming that the crewed deflection mission is failed or aborted. The entry velocity of the CEV is 12 km/s, the maximum allowed by the searching software, and may require a skip re-entry depending on CEV requirements. It may also be possible to perform a skip re-entry in order to eliminate the Earth arrival burn and bring the total required ΔV down to approximately 8 km/s.

C. Rendezvous Mission Analysis

This section briefly describes the requirements to send a precursory robotic mission or fueling station to Apophis. The mission design was performed using a similar program being developed for a manned mission analysis. Only fast transfer orbits have been considered in the following analysis. The use of phasing orbits, gravity assist maneuvers, or multiple revolutions around the sun prior to rendezvous have not been considered. More information on possible rendezvous mission for the post 2029 fictive Apophis orbit can be found in Ref. [14]

Launch opportunities were found by searching for the minimum total ΔV for each launch by allowing the arrival date to vary. The results of the search are shown in Figure 9. Examinations of this plot shows several possible launch opportunities in the 2027-2029 date ranges. A summary of the launch opportunities found is shown in Table 6. A total of 6 launch windows were found, however only the first 4 launch windows allows for an arrival date before or during the manned mission.

With two launch opportunities found, a mission length of 180 days, and a ΔV of 12 km/s determined to be the minimum allowable for a manned mission to Apophis, the mission architecture options can be explored. In the following sections, several possible mission configurations will be considered, with the ultimate goal of obtaining a ΔV of at least 12 km/s.

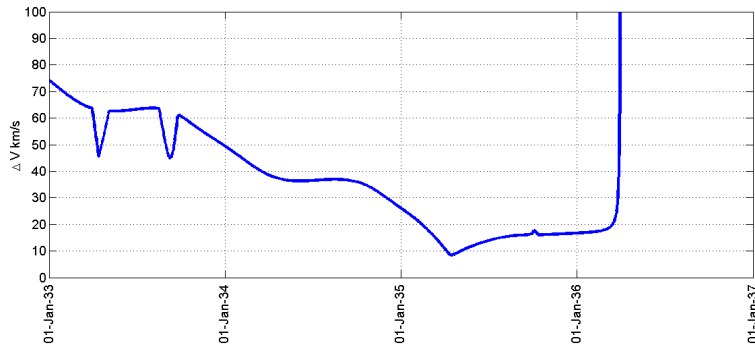


Figure 7. Launch date(2033-2037) versus minimum ΔV required for 360 day crewed deflection mission to the fictive Apophis orbit.

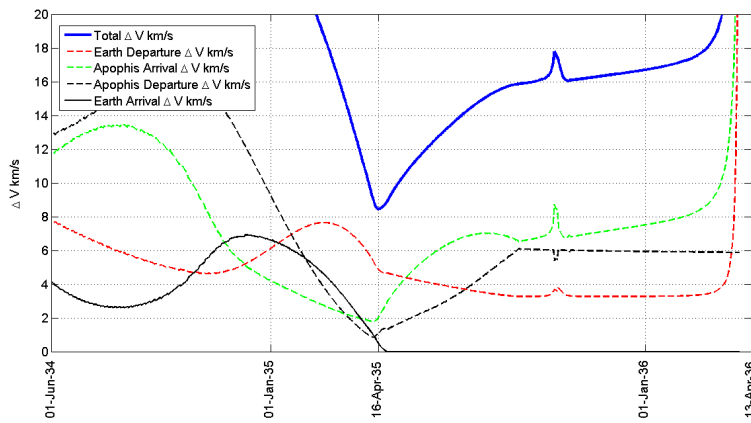


Figure 8. Launch windows found in the 2035-2035 time frame. Plot of launch date versus minimum total ΔV required.

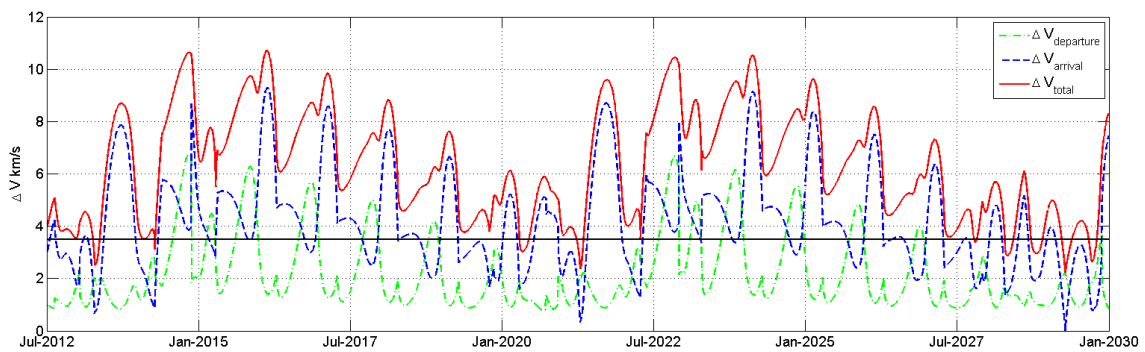


Figure 9. Launch date versus ΔV required for rendezvous mission.

Table 5. Mission information for the 2035 launch opportunity.

Mission Information		Launch 1
Earth Departure		
Date	16-Apr-2035	
C3	38.021	
ΔV (km/s)	4.836	
Apophis Arrival		
Date	3-Mar-2036	
V_{∞}^2	4.185	
ΔV (km/s)	2.046	
Apophis Departure		
Date	13-Mar-2036	
V_{∞}^2	1.254	
ΔV (km/s)	1.120	
Earth Arrival		
Date	15-Apr-2036	
V_{∞}^2	31.569	
ΔV (km/s)	0.435	
Re-Entry V (180 km alt)	12.000	
Totals		
ΔV (km/s)	8.436	

Table 6. Launch and arrival mission information for a single rendezvous mission. Used for the purpose of sending a “fueling station” or precursory robotic mission to Apophis.

Mission Information	Launch-1	Launch-2	Launch-3	Launch-4	Launch-5	Launch-6
Earth Departure						
Date	5/15/2027	10/20/2027	4/30/2028	10/23/2028	4/13/2029	9/23/2029
C ₃	5.062	22.379	14.195	5.425	34.192	25.266
ΔV	0.996	1.741	1.395	1.012	2.224	1.861
Apophis Arrival						
Date	4/12/2028	5/5/2028	2/18/2029	6/23/2029	10/31/2029	7/26/2030
ΔV	2.594	1.640	1.473	1.939	0.019	0.773
Total						
ΔV	3.591	3.381	2.868	2.952	2.243	2.634

III. Mission Architectures

Several possible mission architectures for both the 180 and 365-day missions will be evaluated in this section. A modified Orion CEV will serve as the baseline crew vehicle in each configurations. The Orion specifications obtained from a previous NASA study state that, the Orion CEV has a mass of 20,200 kg for a 21 day lunar mission.¹⁵ This mass is modified for the baseline Orion CEV to account for a 3 person crew and the additional consumables needed for a 180 and 365 day missions. Consumables include food, water, and oxygen which are necessary for the survival of the crew. The baseline Orion CEV mass for this study is developed from the assumption that each crew member requires approximately 8 kg of consumable materials per day.¹⁶ Specifications for the baseline Orion CEV can be seen in Table 7.

Table 7. Orion CEV Characteristics and Performance Capabilities^{16,17}

Endurance	180 Days
Crew Members	3
21-Day Consumables (Four Person)	672 kg
180-Day Consumables (Three Person)	4,320 kg
Mass to Orbit	23,848 kg
Diameter	5.03 m
Habitable Volume	8.95 m ³
Post-EOR ΔV	1.595 km/s
Main Engine Isp	323 s

The current class of heavy launch vehicles includes the Delta IV-H, Atlas V-H, and the Falcon 9-H. Currently only the Delta IV-H is available, so it is the only one used in the architecture configurations shown. The Delta IV-H in this study is primarily used to carry the Orion CEV to LEO. However, the baseline Orion CEV design exceeds the payload capabilities of the vehicle by about 850 kg. The performance of the launch vehicle would need to be improved from its current 23,000 kg to LEO design. A wider fairing would also be necessary due to the diameter of the baseline Orion CEV. A configuration showing three Delta IV-H class launches, requiring no heavy lift Ares V class of rocket, is also shown in Table 8. This configuration assumes that the Orion CEV is launched in one, and two Centaur upper stages are launched in the remaining two. This architecture is shown to illustrate the upper performance limit on the Delta IV-H class of launch vehicle.

Table 8. Listing of ΔV capabilities for possible system architectures. All ΔV 's are in km/s.

Configuration	2-180: ΔV	3-180: ΔV	2-365: ΔV	3-365: ΔV
1 Ares V + Orion	7.028	6.901	6.771	6.530
2 Ares V + Orion	9.430	9.303	9.172	8.932
3 Ares V + Orion	10.751	10.611	10.467	10.200
1 Ares V + Delta IV H + Orion	7.576	7.482	7.386	7.212
2 Ares V + Delta IV H + Orion	9.783	9.678	9.570	9.373
3 Ares V + Delta IV H + Orion	11.159	11.049	10.937	10.731
Ares V NTR + Orion	11.111	10.916	10.715	10.340
Ares V NTR + Delta IV H+ Orion	11.457	11.298	11.135	10.837
1 OTV + Delta IV H + Orion	8.679	8.556	8.432	8.208
2 OTV + Delta IV H + Orion	11.100	10.965	10.828	10.580
3 OTV + Delta IV H + Orion	12.592	12.453	12.311	12.054
3 Delta IV H + Orion	5.921	5.767	5.617	5.359
Orion CEV Masses (kg)	22408	23848	25368	28288

The Ares V launch vehicle is being designed to deliver just under 188 mT to LEO, and makes use of a large Earth departure stage (EDS). The cryogenic EDS uses the J-2X engine, while the massive core stage makes use of six RS-68 derived engines. Two 5.5-segment reusable solid rocket motors (RSRMs) also provide thrust to the core stage. The EDS would be completely exhausted by placing the maximum 188 mT payload into orbit. Propellant can also be left over if the EDS transports a small payload such as the Orion CEV. In this case the additional propellant would be used

during the Earth-departure burn. By using the TLI mass capabilities of the Ares V and the required ΔV to perform the injection, estimates of the remaining LEO propellant can be made.¹⁵ An Ares V carrying the unmodified version of the Orion CEV has an estimated 120 mT of propellant left after delivering the CEV to LEO. The difference in supplies required between the baseline Orion CEV and the unmodified version is then subtracted from the 120 mT to achieve a more refined mass estimate for the usable propellant in LEO. Any architecture which launches an Ares V EDS without a payload, the mass of the baseline Orion CEV is added to the available propellant mass of the EDS in LEO.

Using a cryogenic OTV as the payload for the Ares V can provide better performance capabilities than an EDS because the OTV has a lower dry mass than the EDS. Utilizing the full payload capabilities of the Ares V can allow for a large, modified upper stage to be docked with the Orion CEV. Assuming a burnout mass equal to 10 percent of the total OTV mass, it is reasonable to estimate that a cryogenic OTV could provide around 170 mT of usable propellant in LEO. Three Ares V EDS stages do not provide the upper ΔV limit of 12 km/s, required for the 180-day crewed Apophis mission in the 2028-2029 range. The use of 3 OTVs instead of the EDS is necessary to achieve a total ΔV of 12+ km/s.

In Table 8 an option including a nuclear thermal upper stage is also provided. A nuclear thermal rocket utilizes liquid hydrogen, which becomes super-heated by the thermal energy given off by a fission reaction. The energy density of the hydrogen increases, the hydrogen is expanded through a nozzle to produce thrust. Based on previous research, the I_{sp} performance of such an engine is estimated at around 940 s.¹⁸ In each NTR case, the burnout mass is estimated to be approximately 20 percent of the total upper stage mass. Although normal upper stages have mass ratios of around 10 percent, additional margin is added to account for the inclusion of a space-rated nuclear reactor.

Table 8 shows that producing ΔV capabilities of around 12 km/s requires a very complex system architecture. It may be difficult to accomplish, but the worst-case 180 day crewed Apophis mission is theoretically feasible. However, it should also be noted that propellant boil-off and truss adapters to connect all upper stages are not included in the configuration performances. The inclusion of truss adapters would slightly decrease architecture performance, while propellant boil-off may or may not reduce performance depending on mission length and the burn timing.

While complex mission architectures are required to obtain the ΔV necessary for the 180-day Apophis mission, relatively simple architectures are capable of the 6.5-7 km/s ΔV required for the 1 year mission near the 2029 close encounter. A single launch of the Ares V carrying the Orion CEV is capable of approximately 6.77 km/s ΔV , sufficient for the 2028-2029 1-year missions. If the ΔV margins are not deemed insufficient for the single Ares V launch, a Delta IV-H class launch vehicle could be used to launch the Orion CEV, while the Ares V would launch only the EDS. A 1-year mission would also be ideal to test the feasibility of using the Orion CEV for extended mission as well as other technologies needed for a Mars mission.

The late 1-year mission, in the 2035-2036 date range, requires an architecture capable of producing 9-10 km/s. This number allows extra margin for correction maneuvers, maneuvers while orbiting near Apophis, and possibly lowering the Earth entry velocity. The simplest architecture from Table 8 capable of 9+ km/s ΔV is a 2 person crew utilizing 2 Ares V launches. One Ares V would be used to launch the Orion and an EDS, while the second Ares V would launch an additional EDS.

Several configurations have been found that allow both the 180-day and 1-years mission. The launch vehicles utilized in this section are meant to be representative of launch vehicle classes. The Delta IV-H represents all medium lifting rockets with similar performances, while the Ares V is meant to represent whatever heavy lift rocket is ultimately developed. These configurations will need to be adjusted when a heavy lift rocket becomes available. One of the medium class launch vehicles, the Delta IV-H, Atlas V-H or Falcon 9-H will need to be man-rated as well. However, Table 8 shows that configurations are possible for crewed mission discussed in this paper. The 12 km/s ΔV configurations are the most complex and therefore least likely to be employed.

IV. Conclusion

The ΔV required for a crewed Apophis mission in the 2029 time-frame is significantly reduced as the mission length is allowed to increase. The longest mission length allowed in the recent crewed NEO studies is 180-days. For the crewed Apophis mission this mission length correspond to a total ΔV requirement of 12 km/s. Several mission architectures capable of this high ΔV have been identified in this paper. However, the architectures capable of providing a ΔV of 12+ km/s are complex when compared to lower ΔV configurations. This could be viewed as either an opportunity to test more complex architectures, similar to those likely required for Mars missions, or a reason to extend the mission length out to the 1-year length. Increasing the mission length to 1-year for a crewed mission to Apophis in the 2029 time frame lowers the ΔV requirement for both the early and late launch dates to under 6.5 km/s. It is possible to achieve this performance from a single Ares V class of launch vehicle, making this option much more

desirable.

A crewed mission to a hypothetical Apophis orbit, which will result in an impact on April 13th, 2036, has also been discussed. In this case the only one launch windows was found because the CEV was required to arrive at Apophis prior to impact. This mission would be carried out strictly for a crewed asteroid deflection mission and requires a total ΔV of approximately 8.5 km/s. The minimum mission architecture for this configuration requires the use of 2 Ares V class of launch vehicles.

It appears that a crewed mission to Apophis is feasible with configurations similar to those proposed by the Constellation program. Such a mission requires a longer total mission length to lower the total ΔV requirements. A mission of this length could be used as a step between the first crewed NEO mission in 2025 and the proposed Mars mission in 2035.

Appendix A: Solution to Lambert's Problem

The purpose of this appendix is to lay the ground work necessary to build a computational tool for obtaining the trajectories and results presented in this paper. Several solutions to Lambert's problem have been tested to determine the most efficient solution. Ephemeris data will be needed to calculate the positions of the Earth and each asteroid that is tested.

For any given two position vectors and the time-of-flight (TOF), the orbit determination problem is called Lambert's problem. For this reason Lambert's problem is well suited for an initial orbit determination and searching technique. In Lambert's problem the two position vectors and the TOF are known, but the orbit connecting those two points is unknown. The classical Kepler problem is used to determine a position as a function of time where the initial position and velocity vectors are known. Various solutions so Lambert's problem can be found in the literature.¹⁹⁻²² While many solutions methods have been proposed, three commonly used methods are the classical universal variable method,^{19,21,22} Battin's more recent approach using an alternate geometric transformation than Gauss' original method,^{20,22} and the method developed by Lancaster and Blanchard²³ with improvement and additional details provided by R.H. Gooding.^{24,25} The search for launch dates often requires Lambert's problem to be solved thousands, often millions of time. For this reason the object of this section is to outline the most efficient method to solve Lambert's problem.

A. Lambert Problem Definition

In Lambert's problem the initial and final radius vectors and time-of-flight are given respectively as, \vec{r}_0 , \vec{r} , and Δt . The magnitudes of \vec{r}_0 and \vec{r} are defined as r_0 and r . The following parameters are also needed for the post processing for each solution method.

$$c = |\vec{r} - \vec{r}_0| \quad (1)$$

$$s = \frac{r_0 + r + c}{2} \quad (2)$$

A method to determine the transfer angle $\Delta\theta$ without quadrant ambiguity is described below.²¹ The transfer angle $\Delta\theta$ for a prograde orbit is determined as follows:

$$\Delta\theta = \begin{cases} \cos^{-1}\left(\frac{\vec{r}_0 \cdot \vec{r}}{rr_0}\right) & \text{if } (\vec{r}_0 \times \vec{r}) \geq 0 \\ 360^\circ - \cos^{-1}\left(\frac{\vec{r}_0 \cdot \vec{r}}{rr_0}\right) & \text{if } (\vec{r}_0 \times \vec{r}) < 0 \end{cases} \quad (3)$$

Similarly the transfer angle for a retrograde orbit is determined as:

$$\Delta\theta = \begin{cases} \cos^{-1}\left(\frac{\vec{r}_0 \cdot \vec{r}}{rr_0}\right) & \text{if } (\vec{r}_0 \times \vec{r}) < 0 \\ 360^\circ - \cos^{-1}\left(\frac{\vec{r}_0 \cdot \vec{r}}{rr_0}\right) & \text{if } (\vec{r}_0 \times \vec{r}) \geq 0 \end{cases} \quad (4)$$

B. Battin's Solution

Let's consider Battin's approach first proposed in the 1980's and later published in his book.²⁰ This solution is similar to the method used by Gauss, but moves the singularity from 180° to 360° and dramatically improves convergence when the θ is large. It should also be noticed that Battin's solution works for all types of orbits (elliptical, parabolic, and hyperbolic) just as Gauss's original solution does. Throughout this section a brief outline of Battin's solution will be given. Any details left out can be found in Battin's book.²⁰

1. Geometric Transformation of Orbit

Lambert's problem states that the time-of-flight is a function of a , $r_0 + r$, and c . Therefore the orbit can be transformed to any shape desired as long as the semi-major axis a , $r_0 + r$, and c are held constant. For Battin's formulation^{20,26,27} the orbit is transformed such that the semi-major axis is perpendicular to the line from \vec{r}_0 to \vec{r} , which is c by definition. The geometry of the transformed ellipse is shown in Battin's book.²⁰ From here the equation for the pericenter radius, r_p , is given below. The details leading up to this function can be found in Ref. [20].

$$r_p = a(1 - e_0) = r_{0p} \sec^2 \frac{1}{4} (E - E_0) \quad (5)$$

where e_0 is the eccentricity of the transformed orbit, while r_{0p} is the mean point of the parabolic orbit.²⁰ The mean point of the parabolic radius r_{0p} is also given by:²⁰

$$r_{0p} = \sqrt{r_0 r} \left[\cos^2 \left(\frac{\Delta\theta}{4} \right) + \tan^2 (2w) \right] \quad (6)$$

The value of $\tan^2 (2w)$ is needed for the calculation, which will be defined later. Next Kepler's time of flight equation can be transformed into a cubic equation, which must then be solved. First y will be defined as:

$$y^2 \equiv \frac{m}{(\ell + x)(1 + x)} \quad (7)$$

Kepler's time-of-flight equation can now be represented by the following cubic equation.

$$y^3 - y^2 - \frac{m}{2x} \left(\frac{\tan^{-1} \sqrt{x}}{\sqrt{x}} - \frac{1}{1 + x} \right) = 0 \quad (8)$$

In the above equation l , m , and x are always positive and are defined below. To calculate l , the following two equations, dependent only on the geometry of the problem, are also necessary.

$$\epsilon = \frac{r - r_0}{r_0} \quad (9)$$

$$\tan^2 (2w) = \frac{\frac{\epsilon^2}{4}}{\sqrt{\frac{r}{r_0}} + \frac{r}{r_0} \left(2 + \sqrt{\frac{r}{r_0}} \right)} \quad (10)$$

Using Eqs. (9) and (10), l can be calculated as follows.

$$\ell = \frac{\sin^2 \left(\frac{\Delta\theta}{4} \right) + \tan^2 (2w)}{\sin^2 \left(\frac{\Delta\theta}{4} \right) + \tan^2 (2w) + \cos \left(\frac{\Delta\theta}{2} \right)} \quad 0^\circ < \Delta\theta \leq 180^\circ \quad (11)$$

$$\ell = \frac{\cos^2 \left(\frac{\Delta\theta}{4} \right) + \tan^2 (2w) - \cos \left(\frac{\Delta\theta}{2} \right)}{\cos^2 \left(\frac{\Delta\theta}{4} \right) + \tan^2 (2w)} \quad 180^\circ < \Delta \leq 360^\circ \quad (12)$$

$$m = \frac{\mu \Delta t^2}{8r_{op}^3} \quad (13)$$

$$x = \sqrt{\left(\frac{1-\ell}{2}\right)^2 + \frac{m}{y^2}} - \frac{1+\ell}{2} \quad (14)$$

Initial conditions for x that guarantee convergence are:

$$x_0 = \begin{cases} 0 & \text{parabola, hyperbola} \\ \ell & \text{ellipse} \end{cases} \quad (15)$$

The cubic function (Eq. (8)) can now be solved using the following sequential substitution method:

1. An initial estimation of x is given by Eq. (15).
2. Calculate all the values needed for the cubic from Eqs. (9), (10), (11) or (12), and (13).
3. Solve the cubic Eq. (8) for y .
4. Use Eq. (14) to determine a new value for x .
5. Repeat the above 3 steps until x stops changing.

We now have a nearly complete solution algorithm for Lambert's problem, although solving the cubic function is not a trivial matter. Battin²⁰ next develops a method to flatten the cubic function to improve the convergence rate, as well as a method using continued fractions to determine the largest real positive root of the cubic function. The following section gives the equations necessary to find the flattening parameters and solve the cubic function.

2. Use of Free Parameter to Flatten Cubic Function

The cubic equation, Eq. (8), from the previous section can now be represented in terms of the flattening parameter functions, h_1 and h_2 , as follows:

$$y^3 - (1 + h_1)y^2 - h_2 = 0 \quad (16)$$

The flattening parameters can be represented in terms of x , l , and m as

$$h_1 = \frac{(l+x)^2(1+3x+\xi)}{(1+2x+l)[4x+\xi(3+x)]} \quad (17)$$

$$h_2 = \frac{m(x-l+\xi)}{(1+2x+l)[4x+\xi(3+x)]} \quad (18)$$

The function $\xi(x)$ needed for the calculation of h_1 and h_2 is calculated from the continued fraction as follows:

$$\xi(x) = \frac{8(\sqrt{1+x}+1)}{3 + \frac{1}{5 + \eta + \frac{9}{7\eta} \frac{16}{63\eta} \frac{25}{99\eta} \frac{36}{143\eta} \frac{1}{1 + \dots}}} \quad (19)$$

where η is defined as

$$\eta = \frac{x}{(\sqrt{1+x}+1)^2} \quad \text{where} \quad -1 < \eta < 1 \quad (20)$$

3. Solving the Cubic Function

In this section a method to determine the largest real root of Eq. (16) is outlined. Using this method a successive algorithm can be used ultimately to determine the f and g functions, given by Ref. [19,22]. Using the Lagrangian f and g functions the initial and final velocity vectors are then obtained. The first step is to calculate B and u as follows:

$$B = \frac{27h_2}{4(1+h_1)^3} \quad (21)$$

$$u = \frac{B}{2(\sqrt{1+B}+1)} \quad (22)$$

Also, $K(u)$ is calculated from the continued fraction

$$K(u) = \frac{\frac{1}{3}}{1 + \frac{\frac{4}{27}u}{1 + \frac{8}{27}u}} \quad (23)$$

$$1 + \frac{\frac{2}{9}u}{1 + \frac{22}{81}u}$$

$$1 + \dots$$

where the coefficients for the odd and even coefficients of u are generally obtained from the following two equations.

$$\gamma_{2n+1} = \frac{2(3n+2)(6n+1)}{9(4n+1)(4n+3)} \quad (24)$$

$$\gamma_{2n} = \frac{2(3n+1)(6n-1)}{9(4n-1)(4n+1)} \quad (25)$$

The largest positive real root for the cubic equation is calculated as

$$y = \frac{1+h_1}{3} \left(2 + \frac{\sqrt{1+B}}{1+2u(K^2(u))} \right) \quad (26)$$

The cubic function (Eq. (16)) can now be solved using the following sequential substitution method.

1. An initial estimation of x is given by Eq. (15).
2. Calculate all the values needed for the flattening parameters Eqs.(17) and (18) from Eqs. (9), (10), (11) or (12), and (13).
3. Calculate $\eta(x)$ from Eqs. (19) and (20).
4. Calculate $K(u)$ using Eqs. (21), (22), and (23)
5. Calculate the solution for the cubic function using Eq. (26) for y .
6. Use Eq. (14) to determine a new value for x .
7. Repeat the above 5 steps until x stops changing.

The next step is to determine the semi-major axis of the orbit. If the semi-major axis is positive, the orbit is elliptical, and the initial and final velocity vectors can be calculated as follows. The hyperbolic and parabolic velocity vectors are calculated in a similar manner.²²

$$a = \frac{\mu(\Delta t)^2}{16r_{op}^2xy^2} \quad (27)$$

4. Determining the Lagrange Coefficients for Elliptical Orbits

The Lagrange coefficients for the elliptical orbit case can be calculated from the following set of equations.

$$\beta_e = 2 \sin^{-1} \sqrt{\frac{s-c}{2a}} \quad (28)$$

$$\beta_e = -\beta_e \quad \text{If } \Delta\theta > \pi \quad (29)$$

$$a_{min} = \frac{s}{2} \quad (30)$$

$$t_{min} = \sqrt{\frac{a_{min}^3}{\mu}} (\pi - \beta_e + \sin \beta_e) \quad (31)$$

$$\alpha_e = 2 \sin^{-1} \sqrt{\frac{s}{2a}} \quad (32)$$

$$\alpha_e = 2\pi - \alpha_e \quad \text{If } \Delta t > t_{min} \quad (33)$$

$$\Delta E = \alpha_e - \beta_e \quad (34)$$

The Lagrangian coefficients can be calculated as follows:

$$f = 1 - \frac{a}{r_0} (1 - \cos \Delta E) \quad (35)$$

$$g = \Delta t - \sqrt{\frac{a^3}{\mu}} (\Delta E - \sin \Delta E) \quad (36)$$

$$\dot{g} = 1 - \frac{a}{r} (1 - \cos \Delta E) \quad (37)$$

With the Lagrangian coefficients now known, the initial and final velocity vectors can be found from the following equations.

$$\vec{v}_0 = \frac{\vec{r} - f\vec{r}_o}{g} \quad (38)$$

$$\vec{v} = \frac{\dot{r}\vec{r} - \vec{r}_o}{g} \quad (39)$$

This concludes the solutions to Lambert's problem using Battin's method.

C. Bate, Mueller and White Universal Method

In this section one of the methods used for the multiple revolution Lambert solutions will be presented. This solution is a universal method first proposed by Bate, Mueller, and White¹⁹ and covered extensively in literature.^{21,22,28} Another method, which uses Gooding's^{24,25} extension to the universal method formulated by Lancaster,²³ was used to confirm the result from the BMW method.

In this method the time-of-flight equation can be written as:

$$\sqrt{\mu}t = x^3 S + A\sqrt{y} \quad (40)$$

Where S and C are the Stumpff functions¹⁹ and x , y , and A are:

$$x = \sqrt{\frac{y}{C}} \quad (41)$$

$$y = r_0 + r - \frac{A(1 - zS)}{\sqrt{C}} \quad (42)$$

$$A = \frac{\sqrt{r_0 r} \sin \theta}{\sqrt{1 - \cos \theta}} = \pm \sqrt{r_0 r (1 + \cos \theta)} \quad (43)$$

Where + for a prograde orbit and - for a retrograde orbit.

A plot of the universal time-of-flight equation 40 is shown in Figure 10. The 0-revolution solutions are found in the region up to $4\pi^2$, with the multiple revolution region occurring when z is greater than $4\pi^2$. The regions are bounded by:

$$4n^2\pi^2 < z < 4(n+1)^2\pi^2 \quad (44)$$

The number of complete revolutions is represented by n .

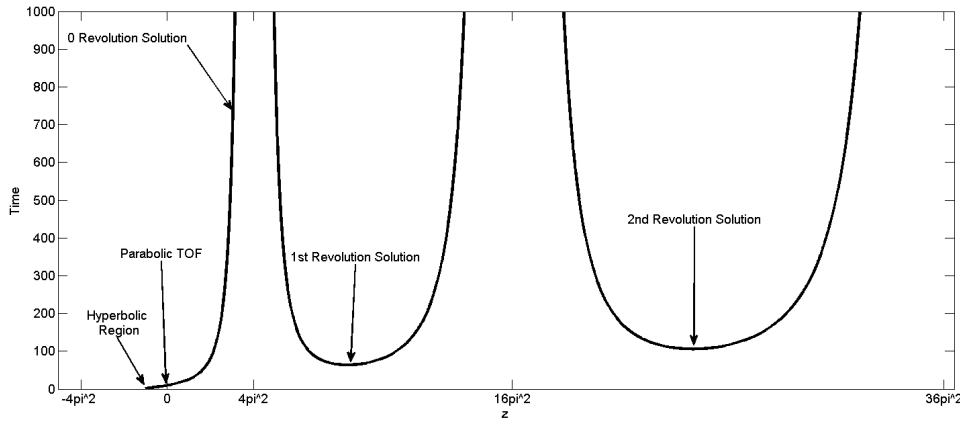


Figure 10. Universal time-of-flight function showing various solution regions.

As Figure 10 indicates there are two solutions for each N -revolution orbits. The left branch is the long-period solution, referred to in this paper as the high-energy solution, with the right branch being the short-period solution, referred to as the low-energy solution. The minimum time-of-flight for a N -revolution orbit can be found by solving the derivative of the time-of-flight equation. The two solution branches can then be solved by root solving the time-of-flight equation. More information on this solution method can be found in BMW¹⁹ and Arora and Russell.²⁸

D. Computational Efficiency for 0-Revolution Solution Methods

In this section an overview of the performance obtained from various Lambert problem solutions will be discussed. The three methods covered in this section are Battin's solution (discussed above), a universal variable using a Newton method, similar to BMW¹⁹ and Curtis,²¹ and lastly a universal variable solution using the bisection method, similar to Vallado.²²

Table 9. Information on the computer used for the computational efficiency study.

Model	Dell T3500 Workstation
Operating System	Windows Vista Enterprise 64 bit
Processor	2 x Intel(R) Xeon(R) W3520 2.67 GHz
Memory	6.00 GB 1066 Mhz DDR3
Matlab	R2009b-64 bit

For all calculations Matlab R2009b (64 bit version) was used. A compile environment would likely increase the general speed of the program, however the program is being written so the final version can be easily used and modified

by others. Table 9 has all the information relevant to the computer used for these calculations. The computer used was a dual quad core Xeon processor (8 total cores) running Windows Vista Enterprise.

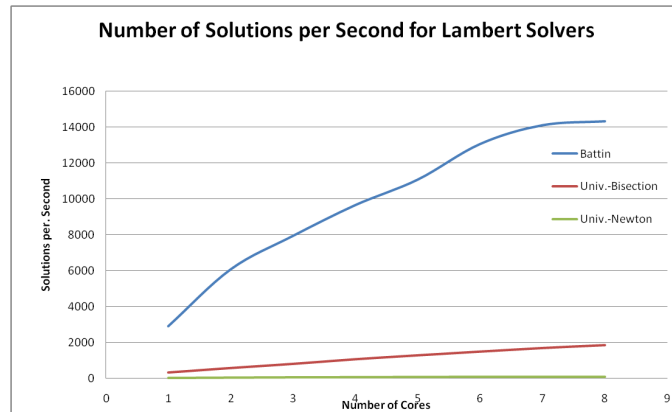


Figure 11. Plot of number of solutions per second versus number of cores for various Lambert solution methods.

In each case the program was run for an example case that is representative of cases that the program would be likely to be used for. In this case it was ran to compute a porkchop plot for an asteroid rendezvous mission. A plot of the number of solutions per second for each of the three solutions is given in Figure 11. Analysis of this plot indicates that the Battin solution is significantly more efficient than either the Newton or bisection solutions. In the same way the Newton universal variable solution is much slower than the bisection method. In general the Newton method would be expected to be more efficient than a bisection method. In this case it is likely that the Newton method doesn't always converge and runs through every loop iteration allowed by the program. On average the Battin solution is 8.94 times faster than the bisection method and 158.66 times faster than the Newton solution method. The maximum number of solutions obtain using all 8 cores (maximum in every case) for the Battin, Newton, and bisection method are 14317, 1867, and 174 respectively.

Appendix B: Main Functions for the Search Program

E. Julian Date

One of the first steps to determine the Earth's, and any other Planet's, orbital elements is to determine the Julian date. Ephemeris data is often given as a function of time, which is represented by the Julian date. The Julian date is number of days that has passed since Jan. 1, 4713 BC 12:00 at Greenwich. The conversion to Julian date from the Gregorian calendar is given by the following equations²¹:

$$JD = J_0 + \frac{UT}{24}$$

where UT is defined to be the number of hours past midnight at Greenwich in decimal form and J_0 is calculated from:

$$J_0 = 367y - INT \left[\frac{7 \left[y + INT \left(\frac{m+9}{12} \right) \right]}{4} \right] + INT \left(\frac{275m}{9} \right) + d + 1721013.5$$

where INT is taken to be the integer value of the number without rounding. The ranges for y , m , and d are:

$$1901 \leq y \leq 2099$$

$$1 \leq m \leq 12$$

$$1 \leq d \leq 31$$

F. Ephemeris Data

To calculate the ephemeris data the Julian date must first be calculated²¹. Once the Julian date is determined, the planetary orbital elements can be calculated from ephemeris tables. The method presented in this section has linear drift rates for each orbital elements, as well as initial values. In this way the orbital elements of each planet can be determined as a function of Julian date. Table (10) shows the drift rates and initial values for Earth²¹. A table with all the information for the other 7 planets and Pluto can be found in Ref. (21).

Table 10. Table of Earths orbital elements and drift rates used to generate ephemeris data.

a, AU	e	i, deg	Ω , deg	$\tilde{\omega}$, deg	L, deg
\dot{a} , AU/Cy *	\dot{e} , 1/Cy	\dot{i} , ''/Cy [†]	$\dot{\Omega}$, ''/Cy	$\dot{\tilde{\omega}}$, ''/Cy	\dot{L} , ''/Cy
1.00000011	0.01671022	0.00005	-11.26064	102.94719	100.46435
-0.00000005	-0.00003804	-46.94	-18228.25	1198.28	129597740.6

* Where Cy is a century, which is 36525 days.

[†] Where '' is symbol for an arcsecond, which 1/3600th of a degree.

The orbital elements are calculated in the following manner. If X is defined to be any of the 6 orbital elements, then the orbital elements can be calculated in the following manner.

$$X = X_0 + \dot{X}T_0 \quad (45)$$

where T_0 , the number of Julian centuries between J2000 and the date, is calculated from the Julian date.

$$T_0 = \frac{JD - 2451545}{36525} \quad (46)$$

$$\omega = \tilde{\omega} - \Omega \quad (47)$$

$$M = L - \tilde{\omega} \quad (48)$$

From the mean anomaly (M) and the eccentricity (e), the eccentric anomaly (E) can be found. Then, the true anomaly (θ) easily can be found. Finding the eccentric angle from M and e requires the Newton iteration method to solve Kepler's time equation, which is described in Curtis²¹.

G. Obtaining the State Vector from Orbital Elements

With all six orbital elements found from the ephemeris routine, the state vector can be calculated. The radius vector is needed for the inputs to Lambert's problem, as well for plotting trajectories. The velocity vectors are also needed to calculate ΔV 's when the each Lambert solution is obtained. The function resulting from this section will be useful in many other situations as well. The first step is to calculate the radius and velocity vectors in the perifocal frame^{21,22}.

$$\vec{r}_{pqw} = \frac{h^2}{\mu} \frac{1}{1 + e \cos \theta} \begin{Bmatrix} \cos \theta \\ \sin \theta \\ 0 \end{Bmatrix} \quad (49)$$

$$\vec{v}_{pqw} = \frac{h}{\mu} \begin{Bmatrix} -\sin \theta \\ e + \cos \theta \\ 0 \end{Bmatrix} \quad (50)$$

Where the specific angular moment, h, is given by

$$h = \sqrt{a(1 - e^2)}\mu \quad (51)$$

The transformation matrix from the perifocal frame to the body centered frame is given by¹³.

$$Q_{pqw \rightarrow ijk} = \begin{bmatrix} \cos \Omega \cos \omega - \sin \Omega \sin \omega \cos i & -\cos \Omega \sin \omega - \sin \Omega \cos \omega \cos i & \sin \Omega \sin i \\ \sin \Omega \cos \omega + \cos \Omega \sin \omega \cos i & -\sin \Omega \sin \omega + \cos \Omega \cos \omega \cos i & -\cos \Omega \sin i \\ \sin \omega \sin i & \cos \omega \sin i & \cos i \end{bmatrix} \quad (52)$$

The radius and velocity vectors in the body centered frame are then transformed by

$$\vec{r}_{ijk} = Q\vec{r}_{pqw} \quad (53)$$

$$\vec{v}_{ijk} = Q\vec{v}_{pqw} \quad (54)$$

H. Obtaining Orbital Elements from State Vector

In this section a method to obtain the six classical orbital elements, a , e , i , Ω , ω , and θ , from the state vector will be discussed. The sixth orbital element is actually, t_p , but this can be obtained directly from θ . This conversion is necessary to propagate orbits and determine the orbital elements after the solution to Lambert's problem has been obtained. All of the following hold true in this section, $r = |\vec{r}|$, $v = |\vec{v}|$, and $h = |\vec{h}|$. The first step is to determine the specific angular momentum vector as follows:

$$\vec{h} = \vec{r} \times \vec{v} \quad (55)$$

The eccentricity vector and orbit eccentricity can be found as

$$\vec{e} = \frac{1}{\mu} \left[\vec{v} \times \vec{h} - \mu \frac{\vec{r}}{r} \right] \quad (56)$$

$$e = |\vec{e}| \quad (57)$$

With the angular momentum and eccentricity now known, the orbit's semi-major axis can be found as

$$a = \frac{h^2}{\mu} \frac{1}{1 - e^2} \quad (58)$$

The inclination of the orbit can be obtained from the angular momentum vector as the inverse cosine of the z component of the angular momentum vector divided by the magnitude of the angular moment. By definition the inclination must be between 0° to 360° , so there won't be any quadrant ambiguities.

$$i = \cos^{-1} \left(\frac{h_z}{h} \right) \quad (59)$$

The node line vector is required to obtain both the right ascension of the ascending node, and the argument of perigee of the orbit. The node line is calculated from

$$\vec{N} = \vec{K} \times \vec{h} \quad (60)$$

$$N = |\vec{N}| \quad (61)$$

The longitude of the ascending node Ω is found from $\Omega = \cos^{-1} \frac{N_x}{N}$, with the proper quadrant, as

$$\Omega = \begin{cases} \cos^{-1} \left(\frac{N_x}{N} \right) & N_y \geq 0 \\ 360^\circ - \cos^{-1} \left(\frac{N_x}{N} \right) & N_y < 0 \end{cases} \quad (62)$$

The argument of perigee and the true anomaly can be found similarly as

$$\omega = \begin{cases} \cos^{-1} \left(\frac{\vec{N} \cdot \vec{e}}{Ne} \right) & e_z \geq 0 \\ 360^\circ - \cos^{-1} \left(\frac{\vec{N} \cdot \vec{e}}{Ne} \right) & e_z < 0 \end{cases} \quad (63)$$

$$\theta = \begin{cases} \cos^{-1} \left(\frac{\vec{e} \cdot \vec{r}}{er} \right) & \vec{r} \cdot \vec{v} \geq 0 \\ 360^\circ - \cos^{-1} \left(\frac{\vec{e} \cdot \vec{r}}{er} \right) & \vec{r} \cdot \vec{v} < 0 \end{cases} \quad (64)$$

I. Solution of Kepler's Time Equation

For the ephemeris routine above a solution to Kepler's time equation is required. In this case both mean anomaly angle, M , and the eccentricity, e , of the orbit are known parameters. A simple solution using Newton's method is presented in this section²¹.

$$M = E - e \sin E \quad (65)$$

The first step for the Newton iteration process is to select an initial value for E .

$$E_0 = \begin{cases} M + \frac{e}{2} & \text{if } M < \pi \\ M - \frac{e}{2} & \text{if } M \geq \pi \end{cases} \quad (66)$$

The Newton process repeats the following two functions until E stops changing within a specified tolerance.

$$\text{error} = \frac{E_i - e \sin E_i - M}{1 - e \cos E_i} \quad (67)$$

$$E_{i+1} = E_i - \text{error} \quad (68)$$

V. Acknowledgments

This work was supported by the Iowa Space Grant Consortium (ISGC) through a research grant to the Asteroid Deflection Research Center at Iowa State University. The authors would like to thank Dr. William Byrd (former Director, ISGC) for his interest and support of this research work.

References

- ¹Korsmeyer, D., Landis, R., and Abell, P., "Into the Beyond: A Crewed Mission to a near-Earth object," *Acta Astronautica*, Vol. 2008, No. 63, April 2008, pp. 213–220.
- ²Landis, R., Abell, Pauland Korsmeyer, D., Jone, T., and Adamo, D., "Piloted Operations at a Near-Earth Object (NEO)," *Acta Astronautica*, Vol. 2009, No. 65, June 2009, pp. 1689–1967.
- ³Landis, R., Korsmeyer, D., Abell, P., and Adamo, P., "A Piloted Orion Flight to a Near-Earth Object: A Feasibility Study," NASA, 2001.
- ⁴O'Leary, B., "Mining the Apollo and Amor Asteroids," *Science*, Vol. 197, No. 4301, July 1977, pp. 363–366.
- ⁵Orloff, R., "Apollos by the Numbers," *U.S. Government Printing Office*, 2001, pp. 256–257.
- ⁶Smith, "A Manned Flyby Mission to [433] Eros," *Northrup Space Laboratory*, Feb. 1966.
- ⁷T, J., "The Next Giant Leap: Human Exploration and Utilization of Near-Earth Objects," *ASP Conference Series*, Vol. 272, 2002, pp. 2003–2013.
- ⁸T D, J. and all, "Human Exploration of Near-Earth Asteroids. In Hazards Due to Comets and Asteroid," *University of Arizona Press*, 1994, pp. 683–708.
- ⁹Wagner, S. and Wie, B., "A Crewed 180-Day Mission to Asteroid Apophis in 2028-2029," *60th International Astronautical Congress*, Vol. IAC-09, No. D2.8.7, Oct. 2009.
- ¹⁰Wagner, S. and Wie, B., "Target Asteroid Selection for Human Exploration of Near Earth Objects," *AAS*.
- ¹¹Giorgini, J., Benner, L., Ostro, S., Nolan, M., and Busch, M., "Predicting the Earth encounters of 99942 Apophis," *ScienceDirect*, Vol. Icarus.
- ¹²NASA, "99942 Apophis (2004 MN4)," *JPL Small-Body Database Browser*, 2010.
- ¹³Wie, B., *Space Vehicle Dynamics and Control*, American Institute of Aeronautics and Astronautics, Inc., Reston, VA 20191, 2nd ed., 2008.
- ¹⁴Wagner, S. and Wie, B., "Design of Fictive Post-2029 Apophis Intercept Mission for Nuclear Disruption," *to be presented at 2010 AIAA Astrodynamics Specialist Conference, Toronto, Canada*, Aug. 2010.
- ¹⁵Creech, S., Sumrall, P., and Cockrell, C., "Ares V Overview and Status," *60th International Astronautical Congress*, Vol. IAC-09, No. D2.8.1, Oct. 2009.
- ¹⁶Korsmeyer, David et al., "Constellation Enabled Mission: Human Exploration of Near Earth Objects," *NASA Advisory Council Briefing*, July 2009.
- ¹⁷"Orion Crew Exploration Vehicle," *NASA, Constellation*, Vol. 2008.
- ¹⁸Davis, E. W., "Advanced Propulsion Study," Tech. Rep. AFRL-PR-ED-TR-2004-0024, Air Force Research Lab and Warp Drive Metrics, Feb. 2004.
- ¹⁹Bate, R., Mueller, D., and White, J., *Fundamentals of Astrodynamics*, Dover Publications, Inc., 180 Varick Street, New York, NY, 1st ed., 1971.
- ²⁰Battin, R., *An Introduction to the Mathematics and Methods of Astrodynamics, Revised Edition*, AIAA Educational Series, 1801 Alexandria Bell Drive, Reston, VA, revised edition ed., 1999.
- ²¹Curtis, H., *Orbital Mechanics for Engineering Students*, Elsevier Butterworth-Heinemann, Linacre House, Jordan Hill, Oxford, 1st ed., 2005.
- ²²Vallado, D., *Fundamentals of Astrodynamics and Applications*, Microcosm Press, 401 Coral Circle, El Segundo, CA, 2nd ed., 2004.
- ²³Lancaster, E. and Blanchard, R., "A Unified Form of Lambert's Theorem," *NASA Technical Note*, Sept. 1969.

- ²⁴Gooding, R., "On the Solution of Lambert's Orbital Boundary-Value Problem," *Royal Aerospace Establishment*, Apr. 1988.
- ²⁵Gooding, R., "A Procedure for the Solution of Lambert's Orbital Boundary-Value Problem," *Kluwer Academic Publishers*, Jan. 1990.
- ²⁶Loechler, L., *An Elegant Lambert Algorithm for Multiple Revolution Orbits*, Master's thesis, Massachusetts Institute of Technology, May 1988.
- ²⁷Shen, H. and Tsiotras, P., "Using Battin's Method to Obtain Multiple-Revolution Lambert's Solutions," *American Astronautical Society*, Vol. 116, 2003.
- ²⁸Arora, N. and Russell, R., "GPU Accelerated Multiple Revolution Lambert Solver for Fast Mission Design," *AAS*, Vol. 10.